THE ASTROPHYSICAL JOURNAL, 546:338–344, 2001 January 1

INTERSTELLAR X-RAY ABSORPTION SPECTROSCOPY OF OXYGEN, NEON, AND IRON WITH THE *CHANDRA* LETGS SPECTRUM OF X0614+091

FRITS PAERELS,[1,2] A. C. BRINKMAN,[2] R. L. J. VAN DER MEER,[2] J. S. KAASTRA,[2] E. KUULKERS,[2,6] A. J. F. DEN BOGGENDE,[2] P. PREDEHL,[3] JEREMY J. DRAKE,[4] STEVEN M. KAHN,[1] DANIEL W. SAVIN,[1] AND BRENDAN M. MCLAUGHLIN[4,5]

Received 2000 May 1; accepted 2000 August 23

ABSTRACT

We find resolved interstellar O K, Ne K, and Fe L absorption spectra in the *Chandra X-Ray Observatory* Low-Energy Transmission Grating Spectrometer (LETGS) spectrum of the low-mass X-ray binary X0614+091. We measure the column densities in O and Ne and find direct spectroscopic constraints on the chemical state of the interstellar O. These measurements probably probe a low-density line of sight through the Galaxy, and we discuss the results in the context of our knowledge of the properties of interstellar matter in regions between the spiral arms.

Subject headings: atomic processes — ISM: general — stars: individual (X0614+091) — techniques: spectroscopic — X-rays: stars

1. INTRODUCTION

It has long been acknowledged that X-ray absorption spectroscopy should be a powerful technique to address the physics and chemistry of the interstellar medium (ISM). The X-ray band contains the K spectra of all charge states of the abundant elements from C to Fe, so that the X-ray spectrum simultaneously captures these elements regardless of their ionization state. In addition, the X-ray absorption spectrum is sensitive to the physical and chemical properties of the interstellar medium constituents. The wavelengths and shapes of absorption lines and edges sensitively depend on whether the absorbing atoms are free or bound in molecules and on whether the atoms are in the gas phase or locked in a solid. A first demonstration of the potential of X-ray spectroscopy in this regard was given by Schattenburg & Canizares (1986), who detected absorption by interstellar O and Ne in the *Einstein* Focal Plane Crystal Spectrometer observations of the Crab Nebula and even found weak evidence for the presence of both neutral and singly ionized O along the line of sight. They also found a hint of the expected narrow 1*s*–2*p* absorption line in atomic O.

We obtained a high-resolution spectrum of the bright, relatively unabsorbed low-mass X-ray binary X0614+091 with the Low-Energy Transmission Grating Spectrometer (LETGS) on the *Chandra X-Ray Observatory* with the hope of resolving the soft X-ray line emission that was detected with the *Einstein* SSS (Christian, White, & Swank 1994), and the Solid State Imaging Spectrometers on *ASCA* (White, Kallman, & Angelini 1997). To our disappointment, we find no evidence for narrow emission lines in the current data, which we take to imply that the discrete emission in this source is time variable. Instead, it turns out that the spectrum of X0614+091 is ideal for interstellar absorption spectroscopy: the source is bright, has a featureless intrinsic continuum, and happens to be behind a column density of interstellar matter such that we have optimum contrast at the O K absorption edge. We detect K-shell absorption by interstellar O and Ne, and L-shell absorption by Fe.

2. DATA ANALYSIS

X0614+091 was observed on 1999 November 28, starting at 22:26:07 UT, for 27,390 s. The LETGS has been described in Brinkman et al. (1987, 1997), Predehl et al. (1997), and in Brinkman et al. (2000). Our observation used the Low-Energy Transmission Grating in conjunction with the High-Resolution Camera (HRC-S) microchannel plate detector (Murray et al. 1997). The LETGS has highest sensitivity in the 5–150 Å (0.08–2.5 keV) band, with an approximately constant wavelength resolution of $\approx$0.06 Å. The data were processed by the standard *Chandra* X-Ray Center pipeline and sorted into an image. The spectrum was extracted by placing a rectangular mask along the spectral image and summing the photons in the cross-dispersion direction. Background was determined from rectangular strips parallel to the spectrum and offset in the cross-dispersion direction. Since we will be using only data at wavelengths less than approximately 30 Å, the use of rectangular masks is adequate.

The location of the centroid of the zero-order image was determined, which fixes the zero of the wavelength scale. Pixel numbers were converted to wavelength using the calibration of the wavelength scale derived from the spectrum of Capella (Brinkman et al. 2000). This wavelength scale is currently believed to be accurate to approximately 20 mÅ (status as of 2000 May). The residual uncertainties appear to be determined mainly by remaining small systematic distortions of the spectral image by the detector and possibly the effect of line blending. The data were binned in 0.02 Å bins, and the positive and negative spectral orders were added to enhance the signal-to-noise ratio, especially longward of 20 Å. In this paper, we will not be using absolute fluxes but will base all quantitative conclusions on the shape of the spectrum over narrow spectral ranges only. We therefore ignore the small systematic errors in the absolute

[1] Columbia Astrophysics Laboratory, Columbia University, 538 West 120th Street, New York, NY 10027; frits@astro.columbia.edu.

[2] SRON Laboratory for Space Research, Sorbonnelaan 2, 3584 CA Utrecht, Netherlands.

[3] Max Planck Institut für Extraterrestrische Physik, Postfach 1503, D-85740 Garching, Germany.

[4] Harvard-Smithsonian Center for Astrophysics, 60 Garden Street, Cambridge, MA 02138.

[5] Department of Applied Mathematics and Theoretical Physics, The Queen's University of Belfast, Belfast BT7 1NN, United Kingdom.

[6] Astronomical Institute, Utrecht University, P.O. Box 80000, 3507 TA Utrecht, Netherlands.

fluxes resulting from our reduction procedure, which are associated with spatial variations in the detector efficiency and background rate.

We removed the higher order contributions to the spectrum in the following manner. Starting at the shortest wavelengths, for each wavelength bin $[\lambda_n, \lambda_{n+1}]$, we compute the number of counts in the second order by scaling with the ratio of the grating efficiency in order $m = 2$ to the first-order efficiency, at λ_n. Note that the efficiencies of all other instrument components divide out, with the exception of the detector flat field. These second-order counts are then subtracted from the counts in the interval $2[\lambda_n, \lambda_{n+1}]$. The process is repeated for orders up to $m = 6$; going to higher m does not affect the spectrum below 30 Å anymore because the first-order spectrum decreases steeply shortward of 6 Å. We distribute the higher order counts to be subtracted from the spectrum uniformly over the bins in the wavelength range $m[\lambda_n, \lambda_{n+1}]$. This assumption concerning the wavelength distribution of the higher order counts is justified for what is evidently a smooth continuum spectrum, and it avoids the large amplification of noise that would result from choosing a narrower redistribution. It does artificially degrade the resolution of the estimated higher order spectrum, but since the incident spectrum is very smooth, we will ignore this inaccuracy here.

Figure 1 shows the spectrum between 5 and 30 Å, background-subtracted and higher orders removed. The background amounts to approximately 1.5–1.8 counts bin^{-1} over the range 10–40 Å. The cumulative higher order flux equals the first-order flux at approximately 26 Å and exceeds it at longer wavelengths.

As is evident, we detect no significant line emission. Instead, a number of highly significant absorption features are clearly visible in the spectrum. The absorption features appear in both the positive and negative spectral orders at mutually consistent wavelengths. The features coincide with the K absorption edges in neutral Ne and O, and the $L_{2,3}$ edges in neutral Fe. The O edge is much deeper than a small edge in the instrument and is clearly of interstellar origin. In addition, we detect a narrow feature at $\sim$23.5 Å, which is consistent with the wavelength of the expected 1*s*–2*p* absorption line in neutral atomic O. All these features are consistent with absorption expected from the ISM. In the following section, we will discuss the interstellar absorption spectrum in detail. The deep edge at 6 Å is instrumental and comprises the $M_{4,5}$ edges in the Ir coating of the mirror, and the $M_{4,5}$ edges in the grating material, Au. In addition, we see the $M_{4,5}$ edges from Cs and I in the CsI coating of the detector. All relevant instrumental features are indicated in Figure 1.

Work on the calibration of the effective area of the LETGS is still in progress. Currently, the effective area is not known accurately enough across the entire 5–30 Å band to attempt a quantitative characterization of the overall spectrum. However, we note that a very simple continuum model (a constant flux in units photons $\text{cm}^{-2}\ \text{s}^{-1}\ \text{Å}^{-1}$, absorbed by an interstellar column density of neutral gas of $N_{\rm H} \sim 1.5\text{–}2.0 \times 10^{21}\ \text{cm}^{-1}$) describes the data to within $\approx$20% across the 5–30 Å band. This implies a total unabsorbed flux in our spectrum of $F(5\text{–}30\ \text{Å}) \approx 1 \times 10^{-9}$ ergs $\text{cm}^{-2}\ \text{s}^{-1}$. The spectral shape is very similar to that found in previous observations with *Einstein* (Christian et al. 1994) and *BeppoSAX* (Piraino et al. 1999). The total unabsorbed flux is in the middle of the range of fluxes observed with *Einstein* (when converted to the 0.5–20 keV band quoted by Christian et al. [1994]) and is virtually equal to that

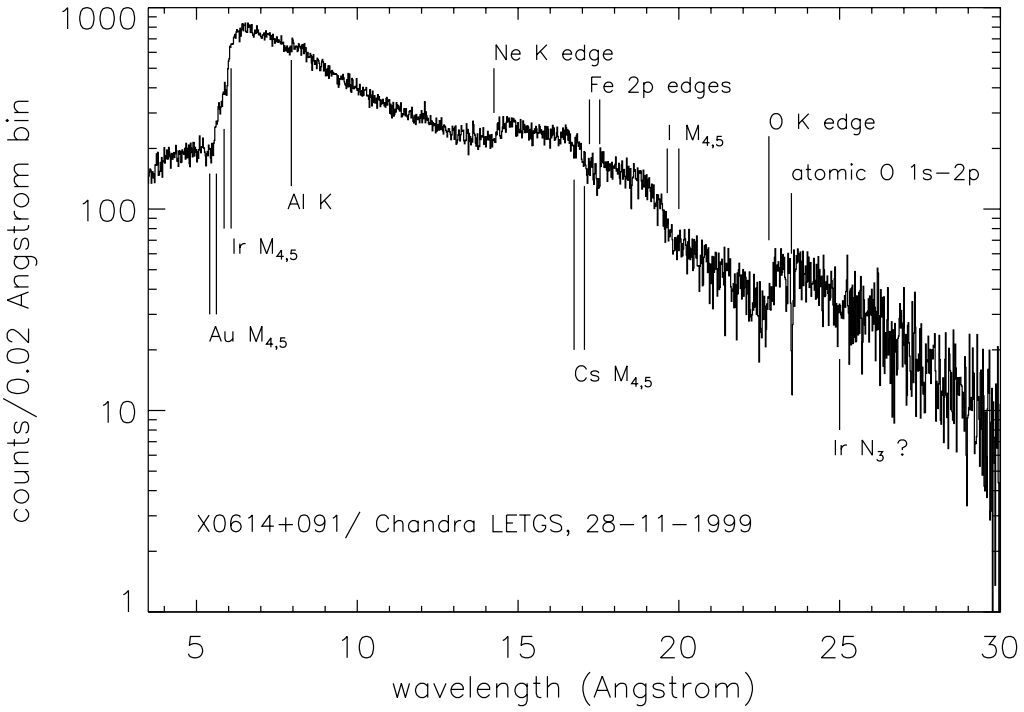

FIG. 1.—Full 3.5–30 Å spectrum of X0614+091, background- and higher order subtracted, binned in 0.02 Å bins. Both positive and negative spectral orders have been summed. Wavelengths of the interstellar Ne K, Fe L, and O K edges have been indicated, as well as the wavelength of the narrow 1*s*–2*p* absorption line in atomic O. Location of known instrumental features (Au, Ir, Al, Cs, and I) has also been indicated. The weak feature at 25Å could be caused by an N-shell resonance in Ir.

observed with *BeppoSAX* (when converted to the *BeppoSAX* 0.1–200 keV band).

3. ABSORPTION BY INTERSTELLAR O, Ne, AND Fe

In Figure 2 we show the spectrum in the wavelength range centered on the O K edge. The counting statistical fluctuations in this range of the spectrum amount to approximately 8 counts bin^{-1} on average, and a cumulative higher order flux of approximately 25 counts bin^{-1} has been removed. A deep edge and a strong narrow absorption line are readily visible, as well as perhaps some additional structure.

There is some structure in the spectrum caused by absorption by O in the UV-Ion Shield (UVIS) on the HRC (Murray et al. 1997). The UVIS comprises a $\sim$800 Å layer of Al on a 2750 Å film of polyimide in the central regions of the detector and a thinner (300 Å) layer of Al at longer wavelengths (beyond $\sim$18 Å). The boundary between the thick and thin Al filters is washed out over an approximately 3 Å wide band because of the dithering of the spacecraft and because the filter is mounted out of focus. The jump in transmission across this region is $\lesssim$10%. The detailed transmission characteristics of the UVIS in the region of the C, N, and O edges were determined from measurements of witness samples undertaken at the BESSY synchrotron facility using a plane grating monochromator with a resolving power $\lambda/\Delta\lambda \sim 2000$—approximately twice that of the LETGS in the same spectral regions. We show the absorption expected from the UVIS explicitly in Figure 2. A shallow, narrow absorption feature appears at $\approx$23.3 Å, as well as an "edge," which gradually rolls over between 22.9 and 23.2 Å, with a relative depth of $\approx$25% (see Fig. 2). The narrow feature is most likely caused by absorption by O bound to N and C in the polyimide, by the analogue of the 1*s*–2*p* transition, while the continuum absorption is caused by all O in the UVIS (polyimide and aluminum oxide). Given the stability of the materials, the transmission curve is not expected to have changed since the ground calibration.

The deep narrow resonance at $\approx$23.5 Å is undoubtedly because of the 1*s*–2*p* absorption line in interstellar monatomic neutral O. Table 1 lists measured and calculated values for the wavelength of this transition. We measured the wavelength from our data by fitting a narrow Lorentzian absorption line, convolved with a Gaussian of width 0.06 Å (FWHM) to represent the response of the LETGS (Brinkman et al. 2000). We find the centroid wavelength to be $\lambda_0 = 23.52 \pm 0.02$ Å, where the error represents the 90% confidence range for one parameter of interest. We take the systematic uncertainty in the wavelength scale into account by adding 0.02 Å in quadrature to this uncertainty. As can be seen in Table 1, our value is consistent with modern experiments (even if the published experimental values do not agree with each other).

McLaughlin & Kirby (1998) calculated the detailed K-shell photoabsorption cross section for atomic O using the ***R***-matrix technique. We use their data to model the absorption by interstellar O. Figure 2 shows the absorption by a column density of O atoms of $N_O = 8 \times 10^{17}$ cm^{-2}. The model spectrum has been shifted by 0.051 Å to match the measured centroid wavelength of the resonance. The continuum model is a simple power law, with interstellar

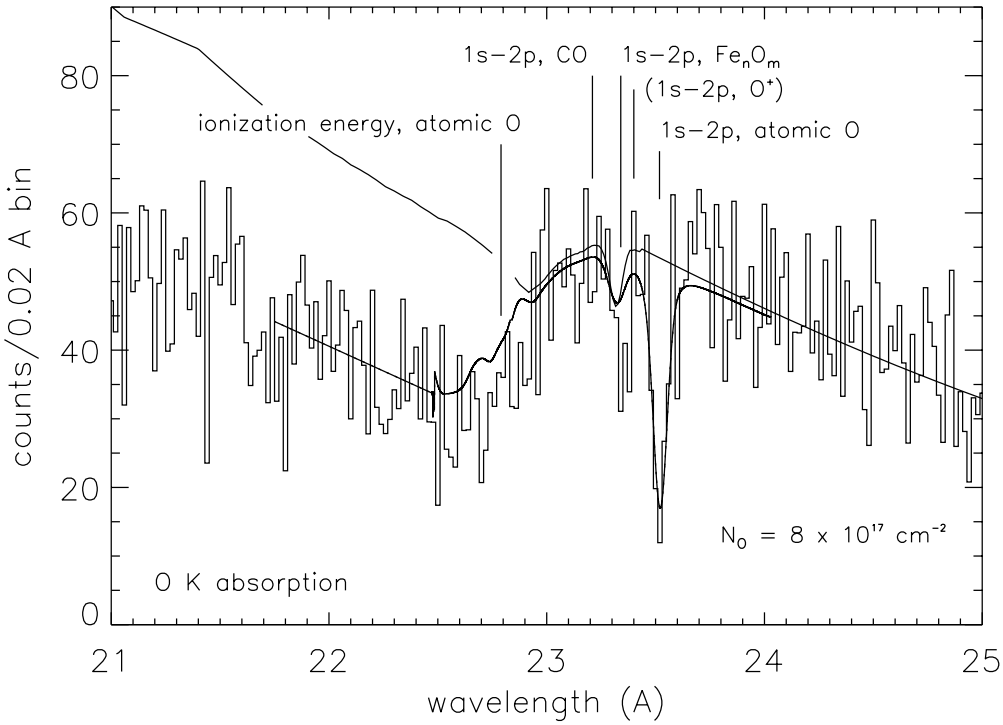

FIG. 2.—The range 21–25 Å in the spectrum of X0614+091. The upper solid line is a simple continuum model, multiplied with the spectrometer effective area (see text). A shallow O K edge is visible at 22.9–23.2 Å, as well as a discrete feature at 23.3 Å caused by the analogue of the 1*s*–2*p* transition in O bound to C and/or N. Both features are caused by the beam filter in the instrument. The lower solid line is the same model but with absorption by a column density of 8×10^{17} neutral O atoms cm^{-2} added. The location of the 1*s*–2*p* analogue in ionized O, CO, and iron oxides has been indicated.

TABLE 1

WAVELENGTHS FOR TRANSITIONS IN ATOMIC OXYGEN

Reference	$1s$–$2p$ (Å)	$1s$–∞ (Å)
Experiment (Krause 1994)	23.489 ± 0.0044	22.775 ± 0.013
Experiment (Stolte et al. 1997).....	23.536 ± 0.0018	22.790 ± 0.002
Experiment (this work)	23.52 ± 0.03	...
Theory (McLaughlin & Kirby 1998)[a]	23.467	(22.775)
Theory (McLaughlin & Kirby 1998)[b]	23.472	(22.790)

[a] ***R***-matrix technique, with the energy of the series limit adjusted to 544.40 eV.
[b] ***R***-matrix technique, with the energy of the series limit adjusted to 544.03 eV.

absorption by elements other than O modeled with the cross sections given by Morrison & McCammon (1983). The entire model spectrum is multiplied with the effective area of the LETGS before convolution with the instrument response.

The measured column density of O, $N_{\rm O} \approx 8 \times 10^{17}$ cm^{-2}, implies that the absorption line is saturated: the optical depth at line center is $\tau_0 \approx 40$ (the line is not resolved by the spectrometer). Unfortunately, that means that the line depth or equivalent width are insensitive to the column density of atomic O. The depth and shape of the K edge are reasonably well represented by the model, but there appears to be some additional absorption near the edge (22.7–23.0 Å), and there is marginal evidence (3–4 σ) for a narrow absorption feature at $\approx$23.4 Å, which could be because of absorption by ionized O, or O in molecules or dust.

Wavelengths for the narrow resonance in CO, various iron oxides, and in singly ionized O are listed in Table 2. As expected, these wavelengths are offset from the wavelength of the resonance in atomic O by a few parts in 500, roughly the ratio of the $n = 2$ binding energy per valence electron to the $1s$ binding energy. We also list the $1s$ binding energy for neutral and singly ionized O. There is no obvious absorption edge caused by O^+ shortward of the neutral O ionization limit, and we place a rough upper limit of $\tau_{O^+} \lesssim 0.2$ on the optical depth in the O^+ continuum. Assuming that the K-shell photoionization cross sections for O and O^+ are approximately equal, this implies $N_{O^+} \lesssim 6 \times 10^{17}$ cm^{-2}. It should be noted that the wavelengths for the transitions in O^+ listed in Table 2 were obtained from approximate atomic structure calculations, and they could be in error by up to of order 1%, or 0.25 Å.

TABLE 2

WAVELENGTHS FOR TRANSITIONS IN ATOMIC AND MOLECULAR OXYGEN

Transition	Wavelength (Å)	Width[a] (Å)	Reference
$1s$–$2p$, atomic O.....	23.467	0.0082	1
$1s$–$2p$, O^+.....	23.40	...	2
$1s$–$2p$, CO	23.21	0.07	3
$1s$–$2p$, FeO	23.31	$\sim$0.1	4
$1s$–$2p$, Fe_2O_3	23.36, 23.31	$\sim$0.1	4
$1s$–$2p$, Fe_3O_4	23.29	$\sim$0.1	4
$1s$–∞, atomic O.....	22.78	...	1
$1s$–∞, O^+.....	22.21	...	5

[a] FWHM.

REFERENCES.—(1) McLaughlin & Kirby 1998; (2) Kaastra & Mewe 1993; (3) Barrus et al. 1979; (4) Wu et al. 1997; (5) Verner et al. 1993.

The wavelengths listed in Table 2 indicate that we can exclude significant absorption by the abundant molecular species CO. This is illustrated in Figure 3, where we show the absorption spectrum caused by a column density $N_{\rm CO} = 2 \times 10^{17}$ cm^{-2} in addition to an atomic column density of $N_{\rm O} = 6 \times 10^{17}$ cm^{-2}. The cross section for CO was taken from Barrus et al. (1979). This combination of column densities was chosen for illustrative purposes only; it produces almost the same continuum absorption as $N_{\rm O} = 8 \times 10^{17}$ cm^{-2} of pure atomic absorption but produces a strong CO resonance feature near 23.2 Å, which is not observed. This absence allows us to place a rough upper limit on the column density of O in CO, of approximately $\lesssim 5 \times 10^{16}$ CO molecules cm^{-2}, as judged by eye. The statistical quality of the spectrum probably does not warrant a more complicated quantitative analysis in this respect.

Interestingly, the feature near 23.4 Å coincides with measured wavelengths for the narrow resonance in iron oxides. Wu et al. (1997) give the relative shapes of the O K absorption spectra in various iron oxides. In addition to the narrow feature at 23.4 Å, the oxides also have deep, broad continuum absorption, with maximum absorption in the range 22.8–23.0 Å. We estimate the depth of the narrow feature to be roughly $\tau_0 \sim 0.5$–1.0. Again, the noise in the data has large enough amplitude that a full quantitative statistical analysis is not warranted. Unfortunately, we are not aware of any quantitative measurements or calculations for the absolute magnitude of the photoabsorption cross section in iron oxide. But if we assume that the total absorption cross section, integrated over the resonance, has the same value as for atomic O and that the line is unresolved, then this line depth corresponds to an equivalent column density of O atoms of $N_{\rm O} \sim 1$–2×10^{16} cm^{-2}. Given the cosmic abundance ratio of Fe to O, $n({\rm Fe})/n({\rm O}) = 5.5 \times 10^{-2}$ (Anders & Grevesse 1989), this result would imply that a major fraction (up to half) of the Fe could be in oxides.

Figure 4 shows the wavelength range between 13 and 19 Å on an expanded scale. In this range are the K edge of Ne and the L edges of Fe. Background is negligibly small compared to the first order flux in this region of the spectrum. The average level of the higher order radiation amounts to 20–30 counts bin^{-1}. We have indicated the locations of the Fe $L_{1,2,3}$ edges, taken from Fuggle & Mårtensson (1980, quoted in Williams 1986; these are binding energies relative to the Fermi level). The $L_{2,3}$ edges are clearly visible in the spectrum. The L_1 ($2s$) edge is expected to be much weaker than the $2p$ edges and indeed is not detected. The Fe L

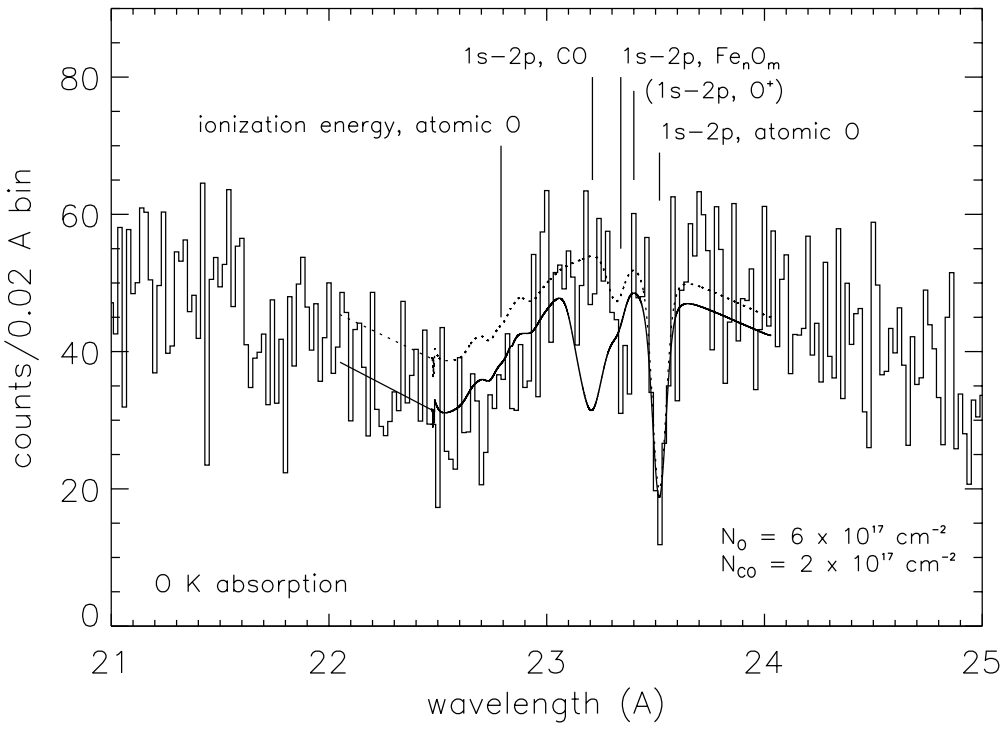

FIG. 3.—As Fig. 2, but with a column density of 2×10^{17} O atoms cm^{-2} replaced by CO (*lower solid line*). A deep discrete feature appears at ~23.2 Å, the analogue of the 1*s*–2*p* transition in O bound to C, which is not seen in the interstellar absorption spectrum of X0614+091. The upper dotted line shows the absorption caused by just the neutral O column density of 6×10^{17} atoms cm^{-2}.

edges are well separated from the instrumental Cs $M_{4,5}$ edges, which are expected to appear in emission (they appear in emission in the featureless continuum spectrum of the quasar 3C273—see J. S. Kaastra et al., 2000, in preparation). The Fe absorption could be caused by metallic iron, iron in molecules, or both. Unfortunately, we have been unable to locate detailed measured absorption cross sections for metallic Fe in the literature.

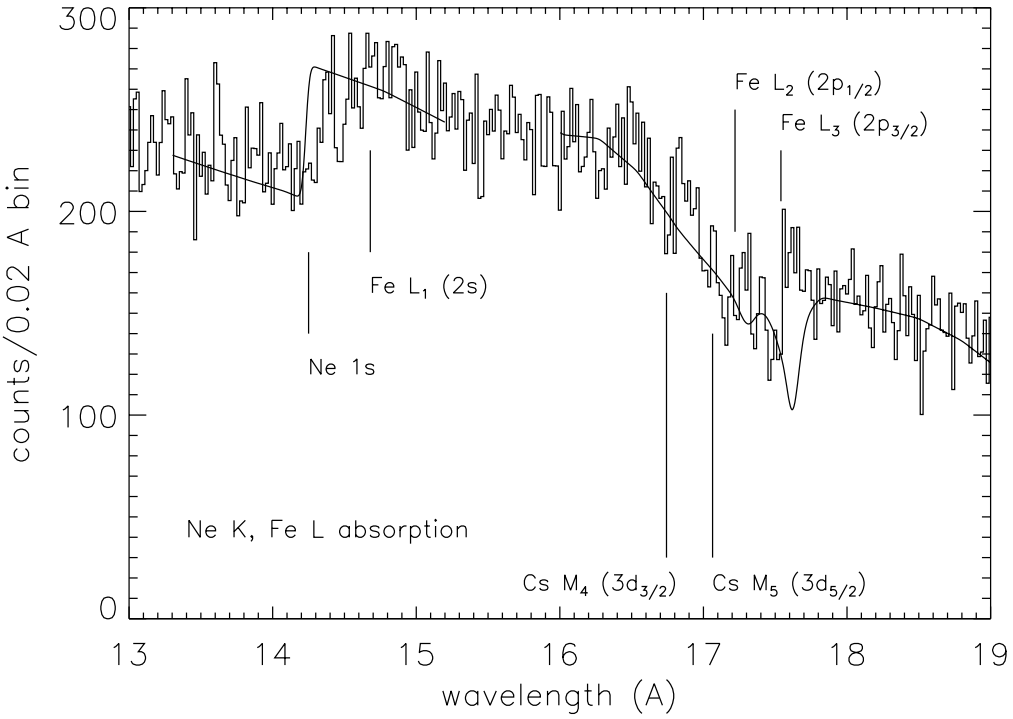

FIG. 4.—The spectral range 13–19 Å, which contains the Ne K and Fe L edges. Solid lines indicate approximate fits to the absorption spectra (see text). Location of the model Ne K absorption edge has been set at the value given by Cardona & Ley 1975. A narrow absorption feature may be present at ≈14.5 Å.

Crocombette et al. (1995) give experimental and theoretical $2p$ absorption spectra for iron oxides (FeO, Fe_2O_3, Fe_3O_4), which we have scaled and superimposed on the data in Figure 4. The general shape of the oxide absorption spectrum is similar to that observed here, except that the measured wavelengths are significantly longer than those observed in our spectrum (by approximately 0.2 Å for all three oxides). We note that a comparison of the positive and negative spectral orders in this limited region seems to indicate a mismatch of about 0.08 Å. The Fe $2p$ features as they appear in Figure 4 are at the average of the positive and negative orders. We caution that this mismatch is larger than any of the wavelength residuals observed in the emission lines in the spectrum of Capella, but it may be just a statistical fluctuation. Taken at face value, the wavelength offset between the Fe oxide absorption spectrum and the Fe $2p$ absorption spectrum observed in our data indicates that (most of) the interstellar absorption is not because of Fe oxides and in fact is consistent with the expected wavelengths for absorption in metallic Fe! This is not consistent with our tentative conclusion from the analysis of the O spectrum that a major fraction of the Fe along this line of sight may be in oxides. A possible explanation is that there is a systematic error on the wavelength scale used by Crocombette et al. (1995), but we are unfortunately in no position to judge the likelihood of this possibility, except to note that the wavelength discrepancy appears large by laboratory experimental standards. In view of the possible small distortion of our wavelength scale, we choose to leave this issue open for now.

Finally, analysis of the Ne K edge is relatively straightforward. We use the cross section given by Verner et al. (1993) to derive a column density of neutral Ne of $N_{\rm Ne} = 1.0 \times 10^{18}$ cm^{-2}, with an estimated uncertainty of about 20%. There is some confusion about the exact ionization energy. Verner et al. (1993) give a wavelength of 14.45 Å for the edge, while Cardona & Ley (1978, quoted in Williams 1986) give 14.25 Å. In our data, the edge actually appears approximately halfway between these two values. There also appears to be some additional structure, a narrow absorption feature at 14.45 Å. This cannot be caused by a narrow $1s$–$2p$ resonance in neutral Ne, because neutral Ne has a closed $n = 2$ shell. A narrow $1s$–$2p$ absorption line in singly ionized Ne is technically possible. Kaastra & Mewe (1993) list 14.38 Å for the wavelength of the $1s$–$2p$ transition in Ne^+, which has a systematic uncertainty of order 1%. However, we do not observe a Ne^+ $1s$ ionization edge, for which Verner et al. (1993) list a wavelength of 14.04 Å. Alternatively, the feature could be the $1s$–$3p$ transition in neutral Ne (compare the K absorption spectrum of neutral Ar in Parratt 1939). Unfortunately, we are not aware of any experimentally determined wavelengths for the K spectrum of Ne^{+0} or Ne^{+1}. In either case, the total depth of the K edge is a reasonable measure of the total column density of Ne along the line of sight.

4. DISCUSSION

We have measured the X-ray absorption spectrum of the interstellar medium along the line of sight to the low-mass X-ray binary X0614+091. We detect the K-absorption spectra of Ne and O and the L absorption spectrum of Fe. The spectra are of sufficiently high resolution and sensitivity that they are sensitive in principle to the physical and chemical state of the ISM. However, our ability to extract the full measure of quantitative information from our data is limited in important respects by the current lack of accurate laboratory measurements or reliable calculations of transition wavelengths and absorption cross sections for the various ions and molecular species of the abundant elements.

The following conclusions are robust, however. We measure a total interstellar oxygen column density of $N_{\rm O} = 8 \times 10^{17}$ cm^{-2}, a fraction of which may be in ionized O or O bound in molecular gas, oxides, or dust. We find that this bound or ionized O cannot all be in CO. We set an upper limit on the fraction of O in CO of $N_{\rm CO}/N_{\rm O} \lesssim 0.06$. Instead, the shape of the spectrum appears consistent with the presence of a significant amount of iron oxide, but this conclusion is not unique, given the limited amount of laboratory comparison spectroscopy. If the narrow resonance feature at $\sim$23.3 Å is indeed caused by iron oxide, we estimate an equivalent column density of O in iron oxide of $N_{\rm O} \sim 1$–2×10^{16} cm^{-2}, i.e., a fraction 1–3 $\times 10^{-2}$ of the atomic O along the line of sight, which would be bound to a major fraction of the available iron.

We measure a total Ne column density of $N_{\rm Ne} = 1.0 \times 10^{18}$ cm^{-2}, which may contain an uncertain fraction of singly ionized Ne. This implies an abundance ratio O/Ne ≈ 0.8, whereas the solar ratio is 6.0 (Anders & Grevesse 1989). The optical depth in the O edge may have been underestimated if we did not subtract enough higher order flux at the O edge. While there are some uncertainties in the calibration of the diffraction efficiencies in the various grating orders, and while we have neglected spatial variations in the detector efficiency, it is unlikely that we have underestimated the depth of the O edge by a factor 6. The discrepancy is also far too large to be ascribed to uncertainties in the photoabsorption cross sections of either O or Ne, which typically run at 20%–30% or less.

A possible astrophysical explanation for the relative shallowness of the O edge would be that a major fraction of the interstellar O along this line of sight is in fact locked up in optically thick dust grains. However, this appears implausible because it would require the dust grains to have an average size of order ~ 1 μm or larger, whereas the characteristic size of galactic dust grains is closer to 0.1 μm, as derived directly from X-ray scattering by interstellar dust (Mauche & Gorenstein 1986; Predehl & Klose 1996). The only other published X-ray absorption spectrum around the O K edge in fact indicates that the dust grains must be transparent to soft X-rays (Schattenburg & Canizares 1986).

In fact, it appears that Ne may be overabundant instead of O being underabundant. If we convert the measured column densities to equivalent H column densities using cosmic abundances, we find $N_{\rm H} \sim 9 \times 10^{20}$ cm^{-2} from the O column density, and $N_{\rm H} \sim 8 \times 10^{21}$ cm^{-2} from the Ne column density. The latter figure is a factor 4–6 larger than the H column density we infer from the overall shape of the spectrum (see § 2), whereas the H column density implied by the O column is within a factor of about 2 of that estimate.

In principle, this apparent overabundance of Ne could be associated with absorbing gas in the binary (a large overabundance of Ne in the general ISM appears very unlikely) or with gas blown out of the binary system. In this context, it is perhaps interesting to note that at least one other low-mass X-ray binary, 4U 1627−67, has also shown a large apparent overabundance of Ne. In the case of 4U 1627−67, this inference is based on the presence of a very bright Ne x

Lyα emission line in the X-ray emission spectrum observed with *ASCA* (Angelini et al. 1995). For now, we defer interpretation of the apparent overabundance of Ne in the absorption spectrum of X0614+091 until after more astrophysical X-ray absorption spectra have become available.

For a low-mass X-ray binary, X0614+091 is located in a somewhat unusual direction: $l_{II} = 200.9°$, $b_{II} = -3.4°$, i.e., more or less in the direction of the Galactic anticenter, a few degrees below the Galactic plane. The distance to X0614+091 has been constrained to $d \lesssim 3$ kpc from the requirement that the inferred peak luminosity during an X-ray burst not exceed the Eddington limit (Brandt et al. 1992). From the reddening of the optical counterpart, Machin et al. (1990) conclude that the source is at least ~ 1.5 kpc away, so that it is located either just at the near edge of the Perseus arm, or inside or behind it (see the recent spiral pattern map in Taylor & Cordes 1993, their Fig. 1). Given the fairly low column density of $N_H = 1 - 2 \times 10^{21}$ cm $^{-2}$, most of the absorption is likely to occur in the low-density environment between the spiral arms, however. The upper limit to the CO column density is not surprising in that case. Note that this region of the sky is just outside the coverage in the deep CO survey of the third galactic quadrant (May et al. 1993). If the source is indeed located on the near side of the Perseus arm, the possible detection of iron oxides, signaling the presence of a non-negligible amount of dust in the interarm region, may be interesting.

We gratefully acknowledge conversations with Jacqueline van Gorkom and a very thorough and helpful reading by the anonymous referee. F. P. acknowledges support from NASA under contract NAS5-31429.

REFERENCES

Anders, E., & Grevesse, N. 1989, Geochim. Cosmochim. Acta, 53, 197
Angelini, L., White, N. E., Nagase, F., Kallman, T. R., Yoshida, A., Takeshima, T., Becker, C., & Paerels, F. 1995, ApJ, 449, L41
Barrus, D. M., Blake, R. L., Burek, A. J., Chambers, K. C., & Pregenzer, A. L. 1979, Phys. Rev. A, 20, 1045
Brandt, S., Castro-Tirado, A. J., Lund, N., Dremin, V., Lapshov, I., & Sunyaev, R. 1992, A&A, 262, L15
Brinkman, A. C., et al. 1987, Astrophys. Lett. Commun., 26, 73
———. 1997, Proc. SPIE, 3113, 181
———. 2000, ApJ, 530, L111
Cardona, M., & Ley, L. 1978, Photoemission in Solids, I: General Principles (Berlin: Springer)
Christian, D. J., White, N. E., & Swank, J. H. 1994, ApJ, 422, 791
Crocombette, J. P., Pollak, M., Jollet, F., Thromat, N., & Gautier-Soyer, M. 1995, Phys. Rev. B, 52, 3143
Fuggle, J. C., & Mårtensson, N. 1980, J. Electron Spectrosc. Relat. Phenom., 21, 275
Kaastra, J. S., & Mewe, R. 1993, A&AS, 97, 443
Krause, M. O. 1994, Nucl. Instrum. Methods B, 87, 178
Machin, G., et al. 1990, MNRAS, 247, 205
Mauche, C. W., & Gorenstein, P. 1986, ApJ, 302, 371
May, J., Bronfman, L., Alvarez, H., Murphy, D. C., & Thaddeus, P. 1993, A&AS, 99, 105
McLaughlin, B. M., & Kirby, K. P. 1998, J. Phys. B: At. Mol. Opt. Phys., 31, 4991
Morrison, R., & McCammon, D. 1983, ApJ, 270, 119
Murray, S. S., et al. 1997, Proc. SPIE, 3114, 11
Parratt, L. G. 1939, Phys. Rev., 56, 295
Piraino, S., Santangelo, A., Ford, E. C., & Kaaret, P. 1999, A&A, 349, L77
Predehl, P., & Klose, S. 1996, A&A, 306, 283
Predehl, P., et al. 1997, Proc. SPIE, 3113, 172
Schattenburg, M. L., & Canizares, C. R. 1986, ApJ, 301, 759
Stolte, W. C., Samson, J. A. R., Hemmers, O., Hansen, D., Whitfield, S. B., & Lindle, D. W. 1997, J. Phys. B: At. Mol. Opt. Phys., 30, 4489
Taylor, J. H., & Cordes, J. M. 1993, ApJ, 411, 674
Verner, D. A., Yakovlev, D. G., Band, I. M., & Trzhaskovskaya, M. B. 1993, At. Data Nucl. Data Tables, 55, 233
White, N. E., Kallman, T. R., & Angelini, L. 1997, in X-Ray Imaging and Spectroscopy of Cosmic Hot Plasmas, ed. F. Makino & K. Mitsuda (Tokyo: Universal Academy Press), 411
Williams, G. P. 1986, in X-Ray Data Booklet, ed. J. Kirz et al. (Berkeley: Lawrence Berkeley Laboratory), 2
Wu, Z. Y., Gota, S., Jollet, F., Pollak, M., Gautier-Soyer, M., & Natoli, C. R. 1997, Phys. Rev. B, 55, 2570